Photo-Fenton Process Using Fe(III) Ions from Modified Sugarcane Bagasse for Reactive Black 5 Dye (RB5) Removal

Aline Rafaela de Almeida* (ID), Christiana Andrade Pessoa (ID), Elaine Regina Lopes Tiburtius (ID), Sérgio Toshio Fujiwara (ID) (*in memorian*)

Brazil is one of the largest generators the sugarcane bagasse, this kind of biomass has already shown efficiency related to its in natura adsorption potential (when physically or chemically activated), it can also be used to remove contaminants from water in methods such as advanced oxidative processes. In this study, chemical modifications were carried out in sugarcane bagasse to enable its application in photo-Fenton processes for the degradation of reactive black 5 dye. The materials were chemically activated through immersion in Fe(III) solution for different periods of time: 3, 6, 9, 12, 24, 48 and 96 h; and were characterized by Fourier transform infrared spectroscopy (FTIR), X-ray diffraction (XRD), zeta potential analysis, internal surface area and leached metal quantification. The results showed the cellulose structure, which is predominant in the sugarcane bagasse it was not considerably modified after activation with $FeCl_3$ and evidence of the presence of Fe(III) ions on the surface of the studied material. The degradation efficiency (after 5 min and using 11.5 mg L^{-1} hydrogen peroxide) for the activated materials was respectively: 55.85%, 49.44%, 71.22%, 92.87%, 88.16% and 98.02%, considering the decrease of the band related to the chromophore group (598 nm).

Graphical abstract
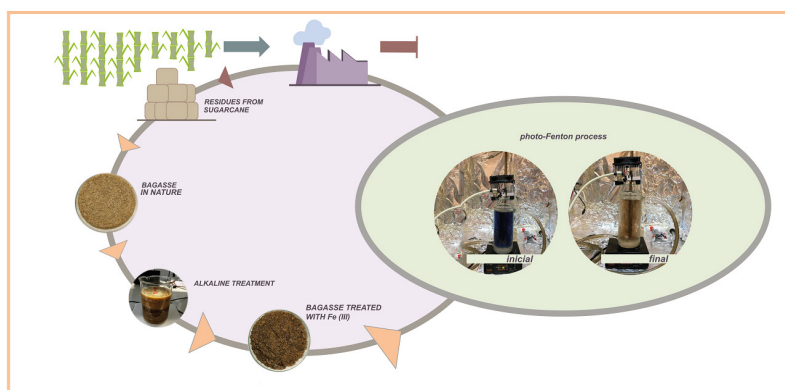
1. Introduction

The wastewater from textile industry produces high effluent quantity and consists in one of the major sources of water contamination by dyes [1]. The amount of reactive dye produced and consumed annually is estimated to be around 80,000 tons [2-5]. Reactive black dye 5 (RB5) is widely used in textile industry due its low cost (around U$ 1.00 g^{-1}), high

Universidade Estadual de Ponta Grossa (UEPG). Programa de Pós-Graduação Doutorado em Química. Avenida General Carlos Cavalcanti, 4748, Bloco L- Uvaranas, Ponta Grossa, Estado do Paraná, CEP: 84030-900, Brazil. *Corresponding author. E-mail: **alinerafaela@hotmail.com**

dyeing power and chemical stability. The azo dye is classified as anionic reactive because it has an electrophilic group capable of forming covalent bonds with the fibers and presents one or more azo groups (-N=N-) attached to aromatic systems. Its high water solubility is due to the presence of a polyaromatic molecule. However, it is resistant to biodegradation under aerobic conditions, which can be highly harmful to both aquatic and human life, considering that its chemical structure can form other carcinogenic and toxic substances [4, 6].

The conventional techniques of effluent treatment, e. g. physicochemical processes, cannot cause azo dye degradation efficiently [7]. For this reason, new technologies, such as advanced oxidative processes (AOPs), have been studied. AOPs are characterized by the degradation of organic species through the hydroxyl radical (•OH) and can partially or totally transform contaminants into other species, such as carbon dioxide, water, inorganic anions, or less toxic substances [8].

The Fenton (Equation 1) and photo-Fenton processes (Equation 2) are the most popular AOPs and have been studied due their simplicity and low cost. The Fenton process uses ferrous ions (Fe^{2+}) as catalysts under acidic conditions to promote the decomposition of H_2O_2 to generate hydroxyl radicals (•OH), which are responsible for the efficiency of contaminant degradation. On the other hand, the photo-Fenton process is assisted by UVB (280-320nm), UVA (320-400 nm) and UV-Vis (400 to 800 nm) irradiation in solution, which promotes an increased formation of •OH radicals. The main advantage of the photo-Fenton process is that it can be assisted by a wide wavelength range and, for this reason, there is the possibility of using sunlight as the radiation source, reducing the cost of the process [9-13].

$$Fe^{+2} + H_2O_2 + H^+ \rightarrow Fe^{+3} + H_2O + \bullet OH \qquad \text{Equation 1}$$

$$Fe(OH)^{+2} + hv \rightarrow Fe^{+2} + \bullet OH \qquad \text{Equation 2}$$
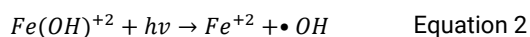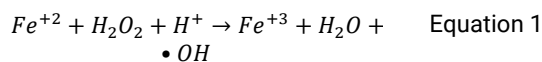
One of the limitations of the photo-Fenton process is that the pH needs to be controlled due to the precipitation of Fe(III) ions above pH 3, and kinetics decrease at pH below 2.5. As an alternative, studies of heterogeneous photo-Fenton processes have been developed by immobilizing Fe(III) ions on organic or inorganic matrices, enabling the reuse of the metal-immobilized material [14]. According to the literature the sugar wastes and chemical modified sugar waste can be used for dyes removal by adsorption. The main advantages of waste from sugar industry is because reduce cost from disposal and environmental protection [1, 8]. The Brazil is one of the countries responsible for the supply of agro-industrial products worldwide, having in this sector one of the main segments of the nation's economy, being significantly important for both domestic supply and exportation [15, 16].The growth and development of the Brazilian agricultural production has increased the production of agro-industrial waste, which has not always been well-managed. According to Law nᵒ 12.305/2010 of the National Solid Waste Policy [17], there is the need to stimulate the elaboration and reformulation of Brazilian public policies and development programs, including the reuse of unused or underused waste such as sugarcane bagasse, which is one of the most produced types of waste in the country [16]. According to the literature, sugarcane wastes (native and chemically modified) can be used for dye removal by adsorption. The main

advantages of using such a kind of waste when developing new methods for dye removal rely on the reduction of cost from disposal and environmental protection [1, 8].

The national production of sugarcane in the 2018/2019 harvest generated 161.31 million tons of sugarcane bagasse. Each ton of sugarcane is estimated to produce about 240-280 kg bagasse, which mostly used for the production of bioelectricity through burning, feeding of cattle after hydrolysis by steam explosion process, and production of second generation ethanol by acidic or enzymatic hydrolysis [18-20].

The chemical composition of sugarcane bagasse consists mainly of natural polymers: cellulose (41 to 44%), hemicellulose (25 to 27%) and lignin (20 to 22%). The other components are oils and greases, ashes, silica and sucrose residues, sugars and polysaccharides (8 to 15%). Cellulose $(C_6H_{10}O_5)_x$, being the main component of the cell wall of all plants, is characterized by its low solubility in water, organic solvents and alkaline solutions, as well as by its resistance to oxidizing agents. Hemicellulose $(C_5H_8O_4)_y$ shows solubility in solvents and reacts with acids, and it is present in sugarcane bagasse mainly as the D-xylan type. Lignin $(C_9H_{10}O_3 (OCH_3))_n$ represents the set of amorphous, cross-linked polymers of high molecular weight and phenolic nature [21, 22]. The sugarcane bagasse chemical structure is characterized by the presence of a high amount of hydroxyls and/or phenolic groups that confer hydrophilic properties for the material. Furthermore, the most reactive groups allow the chemical modification of bagasse to form new compounds with improved properties [23, 24].

Considering the availability of sugarcane bagasse as one of the most common wastes from national agroindustry and their chemical composition, the main objective of this study was to carry out the chemical modification of sugarcane bagasse by basic solution and impregnation with ferric ions for the application in photo-Fenton process for the degradation of reactive black 5 dye.

2. Results and Discussion

2.1 Materials Characterization

The alkali treatment of cellulose can cause changes in its chemical composition [25, 26]. Although Taha et al. [27] claim that the lignin composition remains constant, it was possible to observe in the present work the appearance of brown color during the alkali treatment, which is an evidence of the removal of materials other than cellulose. The concentration of the alkaline solution and the time are important parameters that can control the crystallinity of the material [28-33]. For example, the amorphous parts of the fibers, mainly hemicellulose, lignin and waxes, are dissolved in different extents, and changing the chemical composition can also lead to changed properties. It can be considered that, in this study, the alkaline solution has enabled the removal of amorphous materials and lignin, which has the characteristic of being hydrophobic and amorphous, due to the breaking of the ester bond. Some authors describe that such materials are present mainly near the bagasse surface layer, thus promoting after treatment an increased porosity and internal surface [34-37].

FTIR spectra of the materials were obtained to verify the structural changes of sugarcane bagasse after chemical activation in basic solution and treatment with Fe^{3+} ions. According to the literature, bands in the range from 3600 to 1250 cm^{-1} are responsible for the identification of the most

common groups present in the cellulosic structure and in the interval from 1200 to 600 cm^{-1} correspond to the compound identification fingerprint [38]. Comparing the bagasse before and after the alkaline treatment, it was observed a decrease in the intensity of the bands in the range from 3500 to 2000 cm^{-1}, and from 1500 to 400 cm^{-1}. Additionally, a decrease in the band around 1730 cm^{-1} is evident, which may be due to the break of the carboxylic acid bonds of hemicellulose or even lignin [39]. After the treatment with ferric ions during different times (Figures 1B to 1G), no changes in the spectra were observed. All the spectra presented the characteristic bands of cellulose. The absorption bands at 3396 and 2920 cm^{-1} are ascribed to the stretching vibration of O-H and C-H bonds in polysaccharides. The broad band at 3396 cm^{-1} is due to the stretching vibration of the hydroxyl group, including the ones involved in inter- and intra-molecular hydrogen bonds in cellulose [11]. The band at 2920 cm^{-1} is attributed to C-H stretching of groups from lignin [40, 41]. Typical bands assigned to cellulose were observed in the region of 1607 - 1051 cm^{-1}.

The most common bands found in the literature for *in natura* sugarcane bagasse are presented in Table 1. This initial characterization is important to assess the efficiency of the chemical modification of the material aiming its application in the photo-Fenton process.
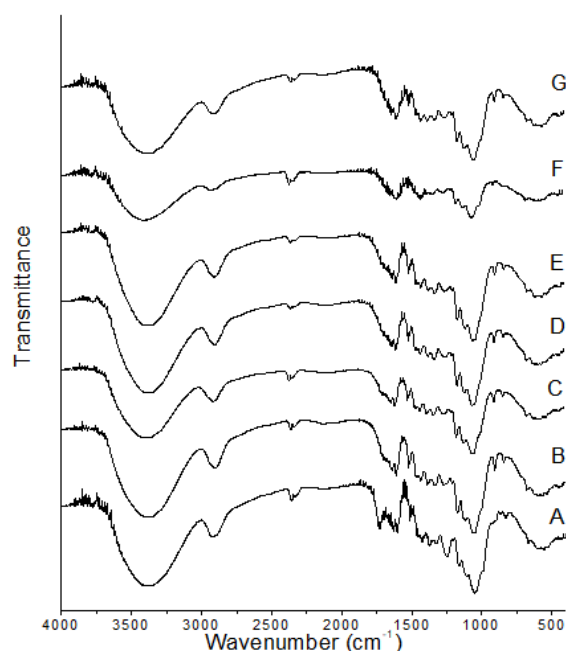

Fig. 1. FTIR spectra from (A) untreated sugarcane bagasse, and bagasse samples treated for (B) 3 h, (C) 6 h, (D) 12 h, (E) 24 h, (F) 48 h and (G) 96 h.

Table 1. Attributions of the main observed FTIR bands of sugarcane bagasse from literature.

Functional group	Wavenumber (cm^{-1})	Assignment	References
O-H	3396	Hydroxyl group (H-bonded) stretching from lignin and cellulose	[40, 41]
C-H	2920	Aliphatic axial deformation from CH$_2$ e CH$_3$ groups of cellulose, lignin and hemicellulose	[42]
O-CH$_3$	2852	Methoxy and C-H stretching of groups in lignin	[40, 41]
C=O	1722	Carboxylic acid stretching	[42, 43]
C=C	1607	Aromatic ring vibration	[44, 45]
C=C	1553	Aromatic ring vibration	[44, 45]
C-O	1242	Lignin and hemicellulose aromatic skeletal vibrations	[46, 47]
O-H	1051	Primary and secondary hydroxyl stretching from cellulose and lignin	[40, 41, 48]
C-O-C	789	Monosaccharide angular deformation	[41]
C-H	573	Aromatic ring stretching	[45]

The alkali treatment loosens up the sugarcane bagasse structure, and this is favored by the presence of water and sodium ions. Such a structural modification can impact the crystallinity of the material. Thus, XRD patterns were obtained for the sugarcane bagasse before and after treatment with Fe(III) ions for different times. The obtained diffractograms are depicted in Figure 2. The scanning angle for XRD was from 5° to 120°, however, from the 80° angle there was no difference in the spectrum due to the amorphous characteristic of hemicellulose and lignin, that is the reason why this region was disregarded for the construction of the graph [48]. The observed peaks correspond to the cellulosic fibers. Specifically, the diffraction peak in the range from 10° to 18° can be ascribed to the presence of cellulose I, which correspond to the amorphous region of cellulose, whereas the peak in the range from 22.2° to 22.7° are due to crystalline forms of cellulose [40, 45, 47].

Both FTIR and XRD results showed no significant change in the cellulose structure, which is predominant in the sugarcane bagasse. Hence, probably most of Fe(III) ions were only adsorbed on the surface of the material. Although the interaction of the metal ions with the material was not evidenced from the characterization results, it is important to emphasize that their adsorption on the material only occurred with the bagasse sample treated with NaOH. On the other hand, experimental results showed that all Fe(III) ions lixiviated from the untreated bagasse when it was immersed in aqueous solution. The strong adsorption of Fe(III) ions on the bagasse surface probably occurred by the formation of iron (III)−cellulose complexes, as described in previous works [49].
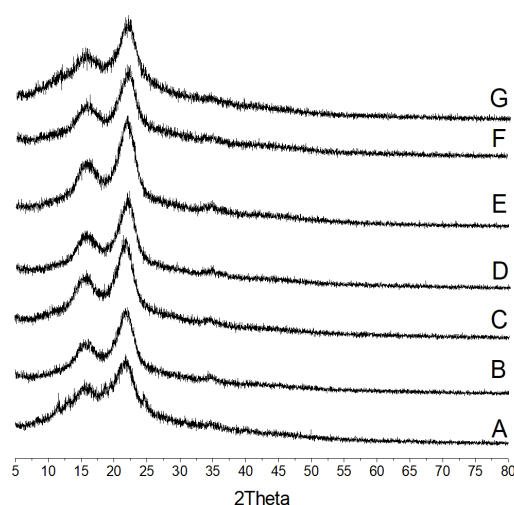

Fig. 2. XRD patterns of (A) untreated sugarcane bagasse, and bagasse samples treated for (B) 3 h, (C) 6 h, (D) 12 h, (E) 24 h, (F) 48 h and (G) 96 h.

The results of zeta potential analysis of the untreated (material A) and activated materials in different times (materials B to F) are presented in Table 2. These measurements revealed that the untreated sugarcane bagasse has a negative potential zeta value that is maintained in different pH ranges, indicating that it has anionic characteristics, which is due to the presence of hydroxyls and carboxylate groups. The anionic features suggest a greater hydrophilic character for the material, which evidences the removal of hydrophobic lignin from the surface [50]. After the bagasse was treated with different concentrations of $FeCl_3$ (materials B to G), the potential zeta values became positive, which is an evidence of the presence of Fe(III) ions on the surface.

Table 2. Potential zeta values of the studied materials: (A) untreated sugarcane bagasse, and bagasse samples treated for (B) 3 h, (C) 6 h, (D) 12 h, (E) 24 h, (F) 48 h and (G) 96 h, in different pH values.

Material	pH3	pH5	pH7	pH10
A	-20.6	-20.1	-5.46	-30
B	7.48	5.48	2.87	1.27
C	6.48	4.58	3.25	2.87
D	5.43	4.21	2.34	1.58
E	4.58	2.56	2.83	1.57
F	8.47	7.96	3.98	0.10
G	-5.02	0.75	0.66	2.68

The results of the internal surface area of the materials are presented in Table 3. There was no significant change in the surface area when comparing the *in natura* sugarcane bagasse with the materials B, D and E. Furthermore, no significant differences were observed regarding the pore diameter, which presented sizes in the nanometric scale. The material C did not follow the described behavior, since it presented a decrease in the surface area and larger pore diameter compared to the other samples, which is characteristic for mesoporous materials. On the other hand, a significant increase in the surface area was showed for the materials F and G.

Table 3. Surface area, pore volume and pore radius of the studied materials: (A) untreated sugarcane bagasse, and bagasse samples treated for (B) 3 h, (C) 6 h, (D) 12 h, (E) 24 h, (F) 48 h and (G) 96 h.

Material	Surface area ($m^2 g^{-1}$)	Pore volume ($cm^3 g^{-1}$)	Pore radius (nm)
A	1.2776	0.0018	1.6604
B	1.1065	0.0025	1.6547
C	0.0231	0.0003	19.9453
D	2.1827	0.0034	1.6522
E	0.8508	0.0020	1.6562
F	21.0049	0.0023	1.6478
G	24.2591	0.0255	1.6599

2.2 Photo-Fenton process

After the characterization, the sugarcane bagasse modified with ferric ions was tested regarding its efficiency towards RB5 degradation by photo-Fenton process, using this material was carried out under similar the experimental conditions describe in the literature using the pH of RB5 and 11.5 mg L^{-1} of hydrogen peroxide, as previously described [11]. Figure 3 shows the results of RB5 degradation percentage after 25 minutes for seven different modified sugarcane bagasse samples (A, B, C, D, E, F and G), whereas Table 4 shows the percentage degradation results acquired every 5 min during the photo-Fenton process.

Comparing the results obtained after 25 min using D, E, F and G materials (Table 4), it is possible to affirm that the RB5 degradation rates reached almost 100%, and no significant difference was observed when comparing these materials. These results showed that a 6-hour immersion of the sugarcane bagasse in Fe(III) solutions was enough to achieve the maximum capacity of immobilization iron in sugarcane bagasse surface. In fact, the most significant differences were observed comparing A, B and C with D, E, F and G samples. Considering the surface area values, it can be observed that this factor was not significant to the degradation results, since the materials F and G (which showed higher surface areas) presented similar degradation rates when compared to D and E. In addition, the results suggest that the pretreatment of the material (D) was important for Fe(III) immobilization, and consequently promoted a higher RB5 degradation efficiency. For instance, a 50% higher degradation rate was observed comparing the results obtained for the material D with the corresponding values observed for materials B and C.
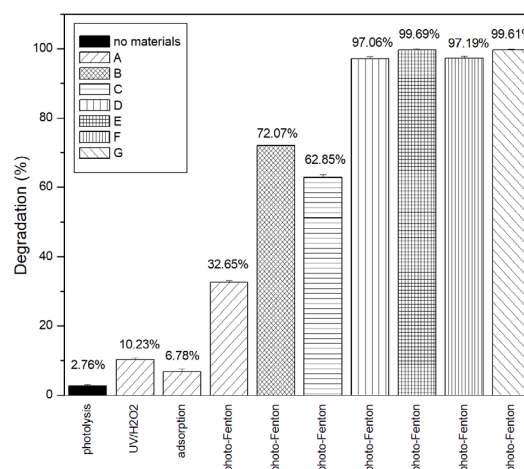

Fig. 3. RB5 (30 mgL^{-1}) degradation rate after 25 min at 25 °C, using 11.5 mg L^{-1} H_2O_2 (initial) and pH = 5.2. Data regarding the photolysis with no materials, UV/H_2O_2 process, adsorption and photo-Fenton with untreated sugarcane bagasse and bagasse samples treated for (B) 3 h, (C) 6 h, (D) 12 h, (E) 24 h, (F) 48 h and (G) 96 h are presented.

Table 4. Degradation rates obtained after different reaction times (5 to 25 minutes) for the investigated materials.

Material	Time (min)				
	5	10	15	20	25
A	21.11 ± 0.21	16.91 ± 0.13	36.20 ± 0.23	12.47 ± 0.15	32.65 ± 0.43
B	55.85 ± 0.17	61.24 ± 0.17	64.63 ± 0.18	68.86 ± 0.24	72.07 ± 0.08
C	49.44 ± 0.18	54.83 ± 0.16	56.21 ± 0.11	59.73 ± 0.08	62.85 ± 0.72
D	71.22 ± 0.14	84.27 ± 0.54	90.87 ± 0.25	94.48 ± 0.23	97.06 ± 0.68
E	92.87 ± 0.12	97.28 ± 0.63	98.26 ± 0.21	99.29 ± 0.16	99.69 ± 0.32
F	88.16 ± 0.22	92.90 ± 0.28	95.51 ± 0.24	96.35 ± 0.52	97.19 ± 0.67
G	98.0 2± 0.07	98.32 ± 0.12	98.62 ± 0.17	99.21 ± 0.34	99.61 ± 0.34

Other processes, such as adsorption, photolysis and UV/H_2O_2 process (Figure 3) might have contributed for RB5 degradation. The observed low photolysis (<3%) was probably due the radiation source, which was a LED UV-Vis lamp that provided radiation in the range from 280 nm to 580 nm, with maximum light emission at 584nm. However, when H_2O_2 was added to the solution, the RB5 degradation rate increased around 7%, and this behavior suggests that degradation mechanisms induced by UV/H_2O_2 process took place in the medium. The removal of RB5 by adsorption was already expected, since previous studies have reported the application of sugarcane bagasse as a biosorbent for azo dyes [51]. However, the low removal rate (<7%) from adsorption evidenced that the photo-Fenton process was predominant during RB5 degradation.

The Fe(III) ions immobilized on sugarcane bagasse increased the hydrogen peroxide decomposition, and consequently enhanced the performance of the process, with high rates of degradation being observed (>95%). Besides that, it is known that the achievement of better degradation results depends on optimized catalyst quantities and reaction conditions [52]. Table 5 shows the amount of ferric ions leached during the photo-Fenton process for all materials used. In all conditions, the Fe(III) ions were leached after 25 minutes. Although the ferric ions were leached after the degradation process, the resulting measured Fe(III) concentrations in all solutions was lower than to 15 mg L^{-1}, which is in the acceptable range for releasing in water bodies, according to the Brazilian law [53].

Table 5. Leached Fe(III) concentrations after RB5 degradation for 25 min via photo-Fenton process: (A) untreated sugarcane bagasse, and bagasse samples treated for (B) 3 h, (C) 6 h, (D) 12 h, (E) 24 h, (F) 48 h and (G) 96 h.

Material	Fe(III) concentration (mg L^{-1})
A	$0.014 \pm 1.85 \times 10^{-4}$
B	$0.038 \pm 6.63 \times 10^{-5}$
C	$0.075 \pm 2.03 \times 10^{-3}$
D	$0.131 \pm 5.18 \times 10^{-4}$
E	$0.271 \pm 2.01 \times 10^{-4}$
F	$2.477 \pm 5.02 \times 10^{-3}$
G	$7.001 \pm 3.24 \times 10^{-4}$

Furthermore, the Fe(III) released suggested that the mechanism of RB5 degradation by photo-Fenton process might be homogeneous and heterogeneous at the same time. According to the literature, three mechanism have been proposed for a heterogeneous process. Firstly, ferric ions are leached into the solution, where the reaction takes place; after that, H_2O_2 decomposes by binding to the metal ions on the surface of catalyst and also via chemisorption of molecule on the catalyst surface [54].The efficiency of dye degradation by using B and C materials was 50% higher than A (lower iron concentration released). These results are interesting because they prove that the sugarcane with immobilized Fe(III) ions can be an alternative support material, and also might promote the slow release of iron, allowing the application of photo-Fenton process at neutral pH. The use of a natural support such as sugarcane bagasse for immobilizing Fe(III) ions opens up new perspectives for treatment of textile effluents mainly due the low cost, simplicity and environmentally friendly nature of the process.

Although, it is difficult compare several AOPs since the efficiency depends on different factors and also conditions the process were carried out such as design reactor, irradiation, dye concentration, iron and hydrogen peroxide concentration and others. The results obtained in this study are in accordance with the literature and also draws the attention to the low hydrogen peroxide concentration used for RB5 degradation. Justino et al. [55] used low amount of H_2O_2 (5.525 mg L^{-1}) in decreasing dosages for the degradation of textile effluents by photo-Fenton process with solar irradiation and obtained a maximum color removal around 67%. Galvão [56] used 1000 mg L^{-1} H_2O_2 in the photo-Fenton process for RB5 dye degradation and obtained a 77.4% removal of chromophore group and 52% removal of aromatic group in 45 min of operation. Glugoski et al. [11] used 100 mg L^{-1} H_2O_2 for 60 min in photo-Fenton dye removal process at pH 3.0 and removed 99.09%. Martins et al. [57] compared the Fenton process, photo-Fenton and UV/H_2O_2 combination for the treatment of textile effluent and obtained the highest efficiency for the photo-Fenton process (95.4%) at pH 3.0. and using 1,500 mg L^{-1} of H_2O_2. Salgado et al. [58] carried out textile effluent discoloration by Fenton and photo-assisted processes at pH 3.0 and 210 mg L^{-1} of H_2O_2, with 99% color removal for the Fenton process; and Lucas and Peres [59] performed Fenton and photo-Fenton processes to degrade RB5 dye and obtained 97.5% and 98.1% removal efficiencies after 15 min, respectively, with pH 3.0 and 33.32 mg L^{-1} H_2O_2 as the optimum conditions.

3. Material and Methods

3.1 Sugarcane bagasse preparation and modification

The *in natura* sugarcane bagasse was initially dried in an oven at 100 ± 10 ºC for 48 h, ground and crushed up to 100 Mesh particle size [60], washed with distilled water and stored for modification and characterization. This sample was named A.

The previously prepared bagasse was modified according to the protocol previously described by Glugoski et al. [11], with modifications. Briefly, the bagasse was mixed with 0.1 mol L^{-1} NaOH solution and heated at 90 °C for 90 min. The bagasse was washed with 0.1 mol L^{-1} H_2SO_4 solution, and deionized water until reaching neutral pH, followed by filtration. The chemically activated resulting material was divided in four parts and immersed in 0.1 mol L^{-1} FeCl$_3$.6H$_2$O solution for the following intervals: 3, 6, 12, 24, 48 and 96 h, under stirring. The modified materials were named B, C, D, E, F and G, respectively. After this step, the materials were washed with distilled water and dried in an oven at 60 ºC.

3.2 Material characterization

FTIR spectra of the materials were obtained by using a Shimadzu IR Prestige-21® spectrophotometer. Analyses were performed in the range from 400 to 4000 cm^{-1}, with 64 scans, at a 4 cm^{-1} resolution. The samples were analyzed by employing KBr pellets containing 1% modified bagasse. XRD analysis was performed by using a Rigaku Ultima IV® diffractometer operating at 40 kV with a 30-mA current and Cu Kα radiation source (λ = 0.1540 nm). The diffraction patterns were registered from 5° to 120° 2θ angle, with a 0.02° step and 1 s sample time. Zeta potential determination was carried out in a Malvern Nano ZS90® instrument. Prior to zeta potential analysis, 0.1 g of each macerated material were suspended and homogenized in 10 mL distilled water. The pH of FeCl$_3$ solution (with initially pH=3.0) was adjusted for each sample;

5.0; 7.0 and 10. Internal surface area was carried out by using the Brunauer-Emmett-Teller (BET) method [61] in a NOVA touch Quantachrome® surface area analyzer. The amount of leached Fe(III) ions from the materials was performed by using flame atomic absorption spectrophotometry. 0.1 g modified material were mixed with 250 mL distilled water in the photo-Fenton reactor. After stirring for 60 min, samples were collected and analyzed in a Varian AA240FS® spectrophotometer, equipped with iron lamp (λ = 258.3 nm), and using an air/acetylene oxidizing flame. The Fe(III) ions leached from the other modified materials were quantified according to methods previously reported [62, 63].

3.3 Photo-Fenton process

The photo-Fenton experiments were performed in a conventional bench-top photochemical reactor equipped with a magnetic stirrer and a light emitting diode (LED) radiation source (50W), as shown in Figure 4.
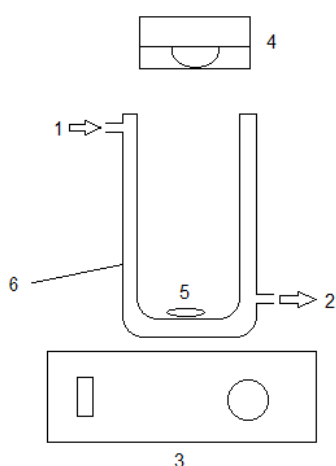

Fig. 4. Schematic of the photochemical reactor:1- Cooling water inlet, 2- Water outlet, 3- Magnetic stirrer, 4- LED located 2 cm away from the reactor, 5- Magnetic bar, 6- 250 mL borosilicate glass container with coupled cooling.

Photo-Fenton degradations were performed with *in natura* and chemically modified sugarcane bagasse samples (A-G). In a typical experiment, 0.2 g bagasse were mixed with 250 mL of a 30 mg L^{-1} RB5 aqueous solution, followed by the addition of 10 μL of 28.78 mg L^{-1} H_2O_2, at pH = 5.2 and 25 °C. The experimental parameters were based on the study reported by Gugloski et al. [11]. , not changing the pH of the RB5 dye solution and reducing the amount of H_2O_2 solution, after some initial experiments of reductions and collection in the time of 5 minutes to observe the degradation over time, starting from the data of that study (100 mg L^{-1}). 6-mL aliquots were collected from the reaction mixture every 5 min until the rection completion in 25 min. In order to evaluate whether the photo-Fenton process was the main degradation mechanism during the performed experiments, photolysis, UV/H_2O_2 and adsorption tests were also performed, maintaining the proportion of solution, material and time to compare the different obtained degradation efficiencies. The experiments were performed in triplicate. All collected aliquots from the reaction mixture were stored in amber glass vials containing 10% $NaHSO_3$. The samples were filtered through a 0.45 μm *Unifil* cellulose acetate filter, and then analyzed in a Varian Cary-50 UV-VIS spectrophotometer. 1 cm optical path quartz cuvettes were used, and the spectra were obtained in the range from 200 to 800 nm. The degradation efficiencies were calculated from the absorbance value at 598 nm (maximum absorption of RB5), by using the following equation:

$$\% \, degradation = \left(a_{i-} \frac{a}{a_i} \right) \times 100 \qquad \text{Equation 3}$$

where a_i is the initial and a is the final RB5 absorbance at 598 nm at the different reaction times.

4. Conclusions

The results obtained in this study showed that sugarcane bagasse can be used as a host matrix for Fe(III) ions, and can be applied as a catalyst in photo-Fenton process to remove dye contaminants. The alkaline treatment of the sugarcane bagasse allowed the removal of part of lignin and other materials. Even after treatment with $FeCl_3$, the structure of the material did not change significantly according to the results obtained from FTIR and XRD experiments. On the other hand, zeta potential and surface area analysis evidenced charge changes in the modified materials, as well as an increase in the internal surface area. It was observed that the immersion time in $FeCl_3$ solution was an important parameter to achieve higher degradation rates. However, it was found that for longer immersion times and greater surface areas, a higher metal leaching was observed, probably due to the larger surface area which does not guarantee that the ferric ions remain attached to the material surface. Therefore, the best degradation results were obtained for the bagasse sample that remained immersed in Fe(III) solution for 12 hours, which also presented the lowest amount of leached metal.

The reported results also show that sugarcane bagasse might be a promising alternative as a support material for Fe(III) adsorption aiming applications in degradation systems that use the photo-Fenton process for the removal of RB5 from water samples. Besides that, the use of a residual and renewable material is highly desirable, since it can provide the degradation of dye contaminants in an ecofriendly and efficient way. However, further studies are necessary to propose an exact degradation mechanism as well as to evaluate the reuse of the studied materials.

Acknowledgments

References and Notes

[1] Ahmad, A.; Khan, N.; Giri, B.; Chowdhary, P.; Chaturvedi, P. *Bioresour. Technol.* **2020**, *306*, 123202. **[Crossref]**

[2] Begum, H. A.; Mondal, A. K.; Muslim, T. *Bangladesh Pharm. J.* **2012**, *15*, 145. **[Crossref]**

[3] Forgacs, E.; Cserha, T.; Oros, G. *Environ. Intern.* **2004**, *30*, 953. **[Crossref]**

[4] Liu, X.; Qiu, M.; Huanga, C. *Procedia Eng.* **2001**, *15*, 4835. **[Crossref]**

[5] Kunz, A.; Peralta-Zamora, P. *Quim. Nova*. **2002**, *25*, 78. **[Crossref]**

[6] Peixoto, F.; Marinho, G.; Rodrigues, K. *Holos*. **2013**, *5*, 98. **[Crossref]**

[7] Anastopoulos, I.; Bhatnagar, A.; Hameed, B. H.; Ok, Y. S.; Omirou, M. *J. Mol. Liq.* **2017**, *240*, 179. [Crossref]

[8] Araujo, K. S.; Antonelli, R.; Gaydeczka, B.; Granato, A. C.; Malpass, G. R. P. *Rev. Ambiente Agua* **2016**, *11*, 387. [Crossref]

[9] Paulino, T. R. S.; Araujo, R. S.; Salgado, B. C. *Eng. Sanit. Ambiental*. **2015**, *20*, 347. [Crossref]

[10] Li, H.; Li, Y.; Xianga, L.; Huanga, Q.; Qiua, J.; Zhanga, H.; Sivaiah, M.V.; Baronb, F.; Barrault, J.; Petit, S.; Valange, S. *J. Hazard. Mater*. **2015**, *287*, 32. [Crossref]

[11] Glugoski, L. P.; Cubas, P. J.; Fujiwara, S. T. *Environ. Sci. Pollu. Res.* **2016**, *26*, 6143. [Crossref]

[12] Xu, T.; Zhu, G.; Zhu, J.; Liang, X.; Zhu, Y.; He, H. *Environmental* **2017**, *212*, 50. [Crossref]

[13] Brillas, E.; Sires, I.; Oturan, M.A.; *Chem. R.* **2009**, *109*, 6570. [Crossref]

[14] Nogueira, R. F. P.; Trovo, A. G.; Silva, M. R. A.; Villa, R. D. *Quim. Nova*. **2007**, *30*, 400. [Crossref]

[15] Spadotto. C.; Ribeiro. W. *Gestão de resíduos na agricultura e agroindústria*. São Paulo: FEFAP, **2006**. Available from: [Crossref] Acess October, 2019.

[16] Available from: [Crossref] Acess October, 2019.

[17] Available from: [Crossref] Acess September, 2019.

[18] Available from: [Crossref] Acess September, 2019.

[19] Available from: [Crossref] Acess September, 2019.

[20] Santos, F.; Borem, A.; Caldas, C. *Cana-de-açúcar-bioenergia. açúcar e etanol:* tecnologias e perspectivas, 2th ed. Viçosa: Editora Universidade Federal de Viçosa, 2013.

[21] Mitrani, R. B.; Sotelo, R. C.; Correa, J. L.; Cadenas, G. A.; Pena, C. G.; Munilla, M. H.; Diaz, M. V.; Rodriguez, N. F. Bagaço. In: *Manual dos derivados da cana-de-açúcar: diversificação, matérias-primas,* derivados do bagaço, derivados do melaço, outros derivados, resíduos, energia. Brasília: ABIPTI, 1999.

[22] Sene, L.; Converti, A.; Felipi, M.G.A.; Zilli, M. *Bioresour. Technol.* **2002**, *83*, 153. [Crossref]

[23] Navarro, R. R.; Sump, K.; Fuji, N.; Matsumura, M. *Water Research*. **1996**, *30*, 2488. [Crossref]

[24] Yamaura, M.1 6 2015 (PI 10011542-6 A2)

[25] Sun, Y.; Cheng, J. *Bioresour. Technol.* **2002**, *83*, 1. [Crossref]

[26] Silva, R.; Haraguchi, S. K.; Muniz, E. C.; Rubira, A. F. *Quim. Nova*. **2009**, 32, 661. [Crossref]

[27] Taha, I.; Steuernagel, L.; Ziegmann, G. *Compos. Interfac.* **2007**, *14*, 669. [Crossref]

[28] Liu, X. Y.; Dai, G. C. Express. *Polym. Lett*. **2007**, 1, 299-307. [CrossRef]

[29] Sawpan, M. A.; Pickering, K. L.; Fernyhough. A. *Compos. Part A Appl. Sci. Manuf*. **2011**, *42*, 888. [Crossref]

[30] Mwaikambo, L. Y.; Ansell, M. P. J. *Mater Sci*. **2006**, *41*, 2483. [Crossref]

[31] Das, M. Chakraborty, D. *J. Appl. Polym. Sci*. **2006**, *102*, 5050. [Crossref]

[32] Gassas, J.; Bledzki, A. K. *J. Appl. Polym. Sci*. **1999**, *71*, 623. [Crossref]

[33] Oushabi, A.; Sair, S.; Hassani, F.O.; Abboud, Y.; Tanane, O.; El Bouari, *South A. J. Chem. Eng*. **2017**, *23*, 116. [Crossref]

[34] Mwaikambo, L. Y.; Ansell, M. P. *J. Mater Sci*. **2006**, *41*, 2497. [Crossref]

[35] Kumar Sinha, A.; Narang, H. K.; Bhattacharya, *S. Mater. Today Proc*. **2017**, *4*, 8993. [Crossref]

[36] Mukherjee, A.; Ganguly, P. K.; Sur, D. *J. Text. Ind*. **1993**, *84*, 348. [Crossref]

[37] Vijav, R.; Lenin Singaravelu, D.; Vinod, A.; Sanjay, M. R.; Siengchin, S.; Jawaid, M.; Khan, A.; Parameswaranpillai, J. *J. Biol. Macromol*. **2019**, *125*, 99. [Crossref]

[38] Holler, F. J.; Skoog, D. A.; Crouch, S. R. Princípios de análise instrumental, 6th ed. Porto Alegre: Bookman, 2009.

[39] Bartos, A.; Anggono, J.; Farkas, A. E.; Kun, D.; Soetaredjo, F. E.; Moczo, J.; A.; Purwaningsih, H.; Pukanszky, B. *Polym. Test.* **2020**, *88*, 106549. [Crossref]

[40] De Oliveira Moutta, R.; Silva, M. C.; Corrales, R. C. N. R.; Cerullo, M. A. S.; Ferreira-Leitão, V. S.; Bon, E. P. S. *J. Microb. Biochem. Technol.* **2013**, *S12*. [Crossref]

[41] Corrales, R. C. N. R.; Mendes, F. M. T.; Perrone, C. C.; Sant` Anna. C.; Souza, W.; Abud, Y.; Bon, E. P. S.; Ferreira-Leitão, V. *Biotechnol. Biofuels*. **2012**, *5*, 36. [Crossref]

[42] Mohomane, S. M.; Motaung, T. E.; Revaprasadu, N. *Materials* **2017**, *10*, 1246. [Crossref]

[43] Reza, R. A.; Ahmaruzzaman, M. *Res. Chem. Intern.* **2015**, *42*, 1463. [Crossref]

[44] Guilherme, A. A.; Dantas, P. V. F.; Santos, E. S.; Fernandes, F. A. N.; Macedo, G. R. *Braz. J. Chem. Eng.* **2015**, *32*, 23. [Crossref]

[45] Phinichka, N.; Kaenthong, G. *J. Mater. Res. Technol.* **2017**, *7*, 55. [Crossref]

[46] Milano, P. A.; Debs, K. B.; Labuto, G.; Carrilho, E. N. V. M. *Environ. Sci. Pollut. Res.* **2018**, *25*, 35895. [Crossref]

[47] Pereira, P. H.; Voorwald, H. C. J.; Cioffi, M. O.; Mullinari, D. R.; Luz, S. M.; Silva, M. L. C. P. *Bioresource* **2011**, *6*, 2471. [Crossref]

[48] Carvalho, W. S.; Martins, D. F.; Gomes, F. R.; Leite, I. R.; Silva, L. G.; Ruggiero, R.; Richter, E. M. *Biomass Bioenergy* **2011**, *35*, 3913. [Crossref]

[49] Kongdee, A.; Bechtold, T. *Carbohydr. Polym.* **2004**, *56*, 47. [Crossref]

[50] Liu, Z. J.; Lan, T. Q.; Gao, X.; Zhang, H. *Bioresour. Technol.* **2017**, *223*, 27. [Crossref]

[51] Tukaram bai, M.; Shaik, O.; Kavitha, J.; Hemanth Varma, M.S.; Chittibabu, N. *Mater. Today Proc.* **2020**, *26*, 842. [Crossref]

[52] Herney-Ramirez, J.; Vicente, M. A.; Madeira, L. M. *App. Catal., B*. **2010**, *98*, 20, 10. [Crossref]

[53] Available from: [Crossref] Access October, 2019.

[54] Pouran, S. R.; Abdul Aziz, A. R.; Daud, W. M. A. W. *J. Ind. Eng. Chem.* **2015**, *21*, 53. [Crossref]

[55] Justino, N. M.; Battistelli, A. A.; Lapolli, F. R.; Lobo-Recio, M. A.; Souza. K. V.; Nagel-Hassemer, M. E. *Eng. Sanit. Ambiental* **2019**, *24*, 33. [Crossref]

[56] Galvão, D. S. Desenvolvimento de um tratamento contínuo de efluente têxtil utilizando filtros de cigarros modificados com íons férricos. Dissertação [Master`s thesis]. Ponta Grossa, Brazil: Departamento de

Química da Universidade Estadual de Ponta Grossa, 2018. **[Link]**

[57] Martins, L. M.; Silva, C. E.; Moita Neto, J. M.; Lima, A. S.; Moreira, R. F. P. M. *Eng. Sanit. Ambiental.* **2011**, *16*, 261. **[Crossref]**

[58] Salgado, B. C. B.; Nogueira, M. I. C.; Rodrigues, K. A.; Sampaio, G. M. M. S.; Buarque, H. L. B.; Araujo, R. S. *Eng. Sanit. Ambiental* **2009**, *14*, 1. **[Crossref]**

[59] Lucas, M. S.; Peres, J. A. *Dyes Pigm*. **2006**, *71*, 236. **[Crossref]**

[60] Di Bernardo, L.; Sabogal Paz, L. P. S; *Seleção de Tecnologias de Tratamento de Água*. São Carlos: LDIBE, 2008.

[61] Brunauer, S.; Emmett, P. H.; Teller, E. *J. Am. Chem. Soc.* **1938**, *60*, 309. **[Crossref]**

[62] Harris, D. C.; Análise Química Quantitativa, 5 th ed. Rio de Janeiro: LTC, 2001.

[63] Atkins, R. C. *J. Chem. Educ.* **1975**, *52*, 550. **[Crossref]**

How to cite this article